

Use of ion implantation to facilitate the discovery and characterization of ferromagnetic semiconductors

N. Theodoropoulou^{a)} and A. F. Hebard

Department of Physics, University of Florida, Gainesville, Florida 32611

S. N. G. Chu

Bell Laboratories, Lucent Technologies, Murray Hill, New Jersey 07974

M. E. Overberg, C. R. Abernathy, and S. J. Pearton

Department of Materials Science and Engineering, University of Florida, Gainesville, Florida 32611

R. G. Wilson

Consultant, Stevenson Ranch, California 95131

J. M. Zavada

Army Research Office, Research Triangle Park, Durham, North Carolina 27709

The discovery of epitaxially grown ferromagnetic, type III–V semiconductors (Ga,Mn)As ($T_c = 110$ K) and (In,Mn)As ($T_c = 35$ K) holds promise for developing semiconductor electronics that utilize the electron's spin degree of freedom in addition to its charge. It has been theoretically predicted that some semiconducting systems could be ferromagnetic above room temperature, when optimally doped (*p*-GaN with 5% Mn). We report here on the use of ion implantation to incorporate magnetic ions into a variety of semiconducting substrates, thereby facilitating investigation of the nature of ferromagnetism in semiconducting systems that are difficult to grow with other methods. The magnetic ions, Mn, Fe, and Ni, were implanted into each of the epitaxially grown semiconductors GaN, GaP, and SiC to achieve volume concentrations between 1 and 5 at. %. The implanted samples were subsequently annealed at 700–1000 °C to recrystallize the samples and remove implant damage. The implanted samples were examined with both x-ray diffraction and transmission electron microscopy to characterize their microstructure and with superconducting quantum interference device (SQUID) to determine magnetic properties. In most cases, no secondary phases were found. The magnetic measurements [hysteresis, coercive fields, and differences between field-cooled (FC) and zero field-cooled (ZFC) magnetizations] indicate ferromagnetism up to room temperature for some samples that could not be attributed to superparamagnetism or any other magnetic phase. Particularly, *p*-GaP:C with high hole concentration, when doped by implantation with 3 at. % Mn, showed ferromagnetic behavior very close ($T_c = 250$ K) to room temperature. In summary, we found that ferromagnetic behavior is very dependent on the concentration of the magnetic impurities for all samples and it is even more dramatically affected by the type and the concentration of the majority carriers, in qualitative agreement with the theory. © 2002 American Institute of Physics. [DOI: 10.1063/1.1452750]

The discovery of diluted magnetic semiconductors (DMSs) has stimulated a strong interest among theorists, because of unusual mechanisms of magnetic behavior, and among experimentalists, because the manipulation of spin in addition to charge promises devices (spin transistors or spin FET's) based on spin polarized transport.^{1–6} Although, II–VI based DMSs have been extensively studied and relatively well understood, DMS materials based on III–V semiconductors have not been as thoroughly investigated. The reason for this is that there is typically low solubility of magnetic ions and, accordingly, difficulty in growing epitaxial samples without formation of secondary phases. Ion implantation provides an alternative way to investigate the nature and the origin of ferromagnetism of DMS materials, especially for those for which a satisfying recipe for epitaxial growth has

not been found. Magnetic ions of Fe, Mn, and Ni were implanted each into GaP, GaN, and SiC at a constant energy of 250 keV designed to produce 3–5 at. % concentration at the peak of the implant profile. TRIM calculations show that the concentration of ions is almost flat for the first 1000 Å of the penetration depth and after 2000 Å it decreases almost linearly to zero at 4000 Å. To avoid amorphization during the implantation step, the samples were held at a temperature of 350 °C. After the implantation, they were annealed at 700–1000 °C for 5 min, under flowing N₂ gas with the implanted area face down. The magnetic properties of all samples were measured in a Quantum Design superconducting quantum interference field-cooled magnetometer and the crystalline quality of the implanted region was examined by transmission electron microscopy (TEM) and selected area diffraction pattern (SADP) analysis. In this article, we will selectively present results on GaN implanted with Fe and Ni, GaP implanted with Mn, and SiC implanted with Fe.

^{a)}Author to whom correspondence should be addressed; electronic mail: nat@phys.ufl.edu

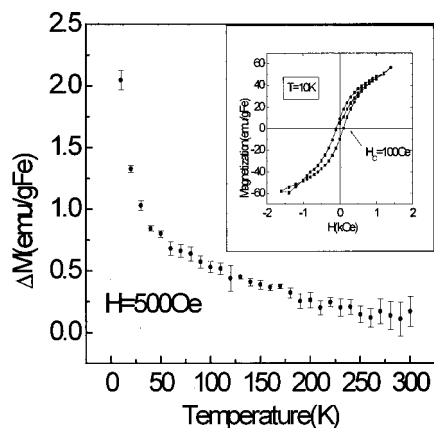


FIG. 1. Temperature dependence of the difference between FC and ZFC magnetization for the *p*-GaN 3 at. % Fe sample. The inset shows the magnetization curve for the same sample at 10 K. A coercive field of 100 Oe was measured.

The GaN samples were grown by metalorganic chemical vapor deposition on Al₂O₃ substrates.⁷ They were doped with Mg and the acceptor concentration was $\sim 2 \times 10^{19} \text{ cm}^{-3}$ with a room-temperature hole concentration of $3 \times 10^{17} \text{ cm}^{-3}$ due to the deep ionization level of the Mg ($\sim 170 \text{ meV}$). Figure 1 shows the difference in magnetization between the field-cooled (FC) and the zero-field-cooled (ZFC) data for *p*-GaN implanted with 3 at. % Fe, and it indicates a ferromagnetic behavior persisting up to room temperature. The difference between the two plots advantageously eliminates para- and diamagnetic contributions and indicates the presence of hysteresis if the difference is nonzero. Although, ferromagnetism is the usual explanation for hysteresis, spin glass effects or superparamagnetism can also be the cause. All of these effects, however, are magnetic phenomena involving the ordering of spins, and it is in that sense that we refer to the hysteresis measured by the FC–ZFC data as ferromagnetic. The inset of Fig. 1 shows the magnetization curve at 10 K. A coercive field of 100 Oe was measured. TEM and SADP analysis did not show any obvious extra spots from secondary phase formation and only the diffraction from the GaN hexagonal crystal structure was observed. The origin of the ferromagnetic behavior in these samples is not clear since the effective hole concentration is certainly less than the initial measured concentration ($3 \times 10^{17} \text{ cm}^{-3}$) present in the starting sample due to implant damage. Theory suggests that much higher hole densities ($> 10^{20} \text{ cm}^{-3}$) are necessary for carrier-mediated ferromagnetism.⁶ The ferromagnetic behavior cannot be attributed to superparamagnetism either since within the TEM resolution (20 Å) there was no aggregation of particles (for Fe a spherical volume of 20 Å radius would imply a superparamagnetic transition temperature of a few Kelvin). A higher concentration of Fe (5 at. %) shows a similar magnetic behavior but in this case the difference between the FC and the ZFC magnetization extrapolates to zero at somewhat lower temperature. The decrease in apparent Curie temperature relative to the 3 at. % Fe implanted GaN sample may be due to a lower hole concentration as a result of more residual implant-induced donor levels. Past work on the electrical effect of implant damage

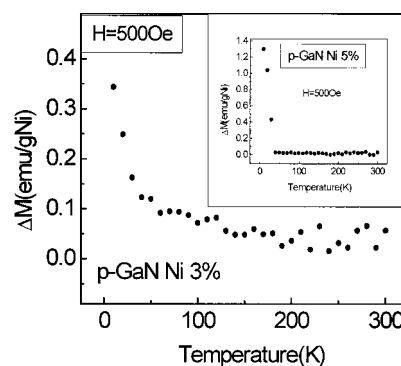


FIG. 2. Temperature dependence of the difference between FC and ZFC magnetization for the *p*-GaN 3 at. % Ni sample. The ferromagnetic behavior persists up to room temperature. The inset shows the same curve for *p*-GaN 5 at. % Ni. The magnetic behavior is different as there is a sharp transition at about 50 K.

in GaN has established its donor nature,⁸ which would reduce the hole concentration in the samples. Another open question is how high levels of Fe incorporation would affect the hole concentration, even in epitaxially grown material. If the Fe has a deep level energy state in the gap with significant capture cross section for the holes, then at room temperature most of the holes in GaN would be trapped at these centers. Since the T_c is expected to be a strong function of both the Fe concentration and the hole density, it would be necessary to have both as high as possible.

The procedures for the growth and the implantation of Ni in GaN as well as the hole concentration were the same as in the case of Fe. Figure 2 shows the difference between the FC and ZFC conditions for the magnetization of *p*-type GaN implanted with 3 at. % Ni. The ferromagnetic behavior for the 3 at. % Ni sample is observed to persist up to 200 K. The inset shows the magnetization for *p*-GaN implanted with 5 at. % Ni. In this case there is a sharp transition at 40 K, indicating a lower hole density compared to the 3 at. % sample due to the implant damage. An unusual shape of the temperature dependence of the magnetization curves for DMSs, similar to Figs. 1 and 2 has been predicted theoretically.^{9–11} According to the theory, it is due to the positional disorder of interacting spins and carriers in doped DMSs that gives rise to a distribution of exchange couplings between Mn ions and holes.

In the case of GaP, Mn was implanted on GaP grown epitaxially on (100) GaP substrates that were doped with C to provide an excess of holes. The samples were consistently characterized as *p* type with a carrier concentration of $2 \times 10^{20} \text{ cm}^{-3}$ at 300 K. Figure 3 shows the temperature dependence of the difference between the FC and ZFC magnetization for GaP doped with 3 at. % Mn. The curve is strikingly different when compared with GaN, and it is very similar to what is predicted by the classical Weiss theory, indicating that the sample is much more ordered than GaNiN and GaFeN. The inset shows a magnetization loop at 250 K. The coercive field was measured to be 100 Oe. Weaker hysteresis was measured at room temperature. It is clear that the ferromagnetic contribution is present above 250 K with an implied Curie temperature of about 270 K which is almost a

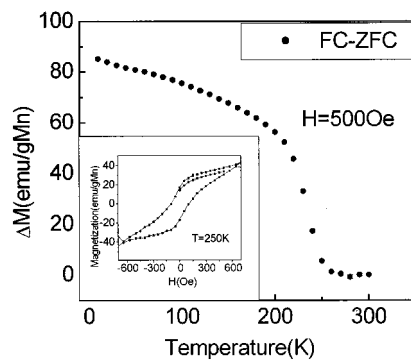


FIG. 3. Temperature dependence of the difference between FC and ZFC magnetization for the *p*-GaP 3 at. % Mn sample. The inset shows the magnetization curve for the same sample at 250 K.

factor of 3 higher than the theoretical prediction of 100 K for GaMnP. The observation of ferromagnetism cannot be due to formation of a MnP phase ($T_c = 290$ K), since TEM and SADP of GaP:C with 3 at. % Mn did not show formation of any secondary phases, only typical residual lattice damage from the implantation. The ferromagnetic behavior of the samples was also very strongly dependent on the Mn concentration. When GaP:C was implanted with 5 at. % Mn the ferromagnetism was heavily suppressed with a transition temperature near 50 K. This result rules out the possibility that the ferromagnetism could be due to the formation of MnP as a secondary phase. The same reduction of ferromagnetism was observed on samples with Mn concentration of 2 at. %, indicating that the 3 at. % Mn is near the “optimal concentration.” In addition, *n*-type GaP samples that were not doped with C during growth, when implanted with 3 at. % Mn, showed a similar suppression of ferromagnetism and appeared to have a critical temperature of about 50 K. These results are in qualitative agreement with the bound magnetic polaron theory.^{12,13} The theory predicts that if the concentration of Mn is more than the optimum concentration, antiferromagnetism will appear. The onset of antiferromagnetism could explain the dramatic decrease in the Curie temperature. It also agrees with the importance of holes as the majority carriers for mediating the Mn–Mn exchange interaction.

Finally, SiC implanted with Fe was studied.¹⁴ Bulk 6H–SiC wafers (Al doped) with a room temperature hole concentration of $\sim 10^{17}$ cm⁻³ were implanted with 250 keV Fe⁺ at doses of $3\text{--}5 \times 10^{16}$ cm⁻³. The implantation and annealing procedure is the same as previously described for GaN and GaP. Figure 4 shows the difference between the FC and the ZFC magnetization for the 5 at. % Fe sample. It is clear that a remnant of ferromagnetic contribution is present even at room temperature. The inset shows the magnetization curve at 10 K for the same sample. We did not observe any secondary phase formation involving the precipitation of Fe or formation of FeC_x or FeSi_x compounds. Moreover, the implanted region was relatively resistive, with capacitance–

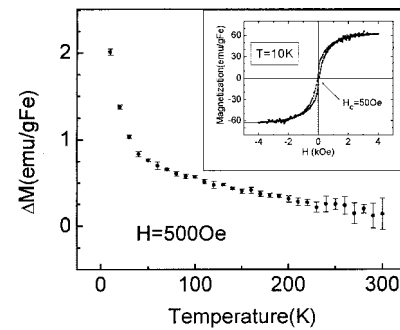


FIG. 4. Temperature dependence of the difference between FC and ZFC magnetization for the SiC 5 at. % Fe sample. The inset shows the magnetization curve for the same sample at 10 K. A coercive field of 50 Oe was measured.

voltage measurements showing depletion beyond the Fe range after the implantation and the annealing process, with the hole concentration being $< 10^{15}$ cm⁻³ in that region. Whether the remaining hole density is sufficient to induce carrier-mediated ferromagnetism in SiC needs additional work to answer, involving substrates of different conductivity level and type. In addition, the material implanted with 3 at. % Fe did not show any signature of ferromagnetism. Since the Curie temperature is predicted to be a strong function of both the hole concentration and magnetic ion concentration in wide band gap dilute magnetic semiconductors, the lower dose samples may be below the threshold for inducing ferromagnetism.

In summary, we have demonstrated that ion implantation provides an opportunity to efficiently create and then screen a wide variety of DMS samples. In addition to enabling a quick determination of the Curie temperature, implantation in different DMS host materials may also have applications in forming selected area contact regions for spin-polarized carrier injection in device structures.

The work at UF is partially supported by NSF, while that of R.G.W. is partially supported by ARO.

¹H. Ohno, *Science* **281**, 951 (1998).

²G. A. Prinz, *Science* **282**, 1660 (1998).

³B. Lee, T. Jungwirth, and A. H. MacDonald, *Phys. Rev. B* **55**, R3347 (1997).

⁴D. D. Awschalom and R. K. Kawakami, *Nature (London)* **408**, 923 (2000).

⁵D. D. Awschalom and J. M. Kikkawa, *Phys. Today* **52**, 33 (1999).

⁶T. Dietl, H. Ohno, F. Matsakura, J. Cibert, and D. Ferrand, *Science* **287**, 1019 (2000).

⁷T. Theodoropoulou, A. F. Hebard, M. E. Overberg, C. R. Abernathy, S. J. Pearton, S. N. G. Chu, and R. G. Wilson, *Appl. Phys. Lett.* **78**, 3475 (2001).

⁸S. J. Pearton, J. C. Zolper, R. J. Schul, and F. Ren, *J. Appl. Phys.* **86**, R1 (1999).

⁹P. A. Wolff, R. N. Bhatt, and A. C. Durst, *J. Appl. Phys.* **79**, 5196 (1996).

¹⁰R. N. Bhatt and X. Wan, *Int. J. Mod. Phys. C* **10**, 1459 (1999).

¹¹R. N. Bhatt and M. Berciu, *cond-mat/0011319*.

¹²T. Dietl and H. Ohno, *Physica E (Amsterdam)* **9**, 185 (2001).

¹³T. Dietl, A. Haury, and Y. Merle d'Aubigne, *Phys. Rev. B* **55**, R3317 (1997).

¹⁴N. Theodoropoulou, A. F. Hebard, M. E. Overberg, C. R. Abernathy, S. J. Pearton, S. N. G. Chu, and R. G. Wilson (unpublished).